The Dhaka University Journal of Earth and Environmental Sciences, Vol. 11 (1): 2022

Shoreline Dynamics Assessment of Moheshkhali Island of Bangladesh using Integrated GIS-DSAS Techniques

Md. Kawsarul Islam[1], Mahmudul Hasan[1]*, Mahfujur Rahman[2], Rafid Fayyaz[1], Masuma Chowdhury[2] and Taspiya Hamid[3]

[1]Department of Oceanography, University of Dhaka, Dhaka 1000, Bangladesh
[2]Department of Geology, University of Dhaka, Dhaka 1000, Bangladesh
[3]Department of Oceanography & Hydrography, Bangabandhu Sheikh Mujibur Rahman Maritime University, Bangladesh

Manuscript received: 19 November 2021; accepted for publication: 31 August 2022

ABSTRACT: Coastal areas of Bangladesh are more susceptible to the adverse effects of climate change due to their geographic location and geological condition. The coastal zones and offshore islands of the country have indisputably experienced the combined consequences of global temperature and sea level rise. Aiming to study and understand shoreline dynamics and shoreline change, medium resolution (30m) satellite imagery over 30 (1990-2020) years was being executed. The Digital Shoreline Analysis System (DSAS) in the GIS platform was used in conjunction with other geospatial techniques to ascertain shoreline dynamics in multiple satellite images taken over this period, and afterward, the spatial outcomes were validated through a detailed field investigation. The study demarcated that the shoreline of Moheshkhali is subjected to severe erosion and accretion and has undergone significant morphological changes. On the basis of average shoreline change rates, the island's shoreline is divided into 6 accretion zones and 4 erosion zones, with accretion being the dominant process. Accretion occurs in the south and south-western parts of the island, particularly those near the sea heads, which have experienced significant accretion at a rate of more than 86 m/yr and the consequent westward and south-east migration of the shore due to the active deposition along the coast. Besides, minor alterations were observed in the north and north-eastern part of the island. The study also evident that climate change, windy storms, variability in coast material, intermittent wave and air action, longshore transport, and anthropogenic activities are prime factors that contribute to the highly dynamic nature of the shorelines of Moheshkhali island. Therefore, this study demonstrates the benefit of using an integrated GIS-DSAS tool to investigate spatiotemporal shoreline change, and it might be valuable in land-use planning and coastal erosion mitigation on Moheskhali Island.

Keywords: Moheshkhali Island; Shoreline; GIS-DSAS; Erosion; Accretion

INTRODUCTION

Global climatic change induces several extreme natural catastrophes like tsunamis, cyclonic storm surges, coastal erosion, and sea surface temperature rise that have dreadful consequences for coastal zones (Islam, et al., 2016b; Islam et al., 2015). Consequently, all of the associated components of the coastal area, most particularly coastal lifestyles, belongings, harbor protection, environmental factors, socioeconomic factors, and land resources, are seriously compromised (Al-Zubieri et al., 2020). Shorelines, the contact between land and sea, are subject to change as a result of sea-level rise, with variances due to a variety of factors, including meteorological, morphological, and geological considerations. Most notably, this is also a prerequisite for acknowledging that natural factors are not the sole driving factors where overpopulation and associated socio-economic, industrial, and infrastructural activities are also contributing.

Likewise, the shoreline in Bangladesh is also rigorously affected by tectonics, sediment transportation, and environmental intervention. They are frequently impacted by natural catastrophes such as cyclones, coastal flooding triggered by storm surges, waterlogging, and erosion (Mallick and Rahman, 2013). Especially sea-level rise is alleged to be a direct consequence of global warming and additionally results in the influx of saline water, transforming fresh water sources (groundwater) to saline (Ali, 1996; Choudhury et al., 1997; Karim and Mimura, 2008). Thus, the development of a sustainable resource management strategy and evaluating shoreline dynamics are indispensable (Islam, et al., 2016a). Considering these, monitoring and assessing the modification of shoreline is primary

Corresponding author: Mahmudul Hasan
Email: mahmud.hasan@du.ac.bd

DOI: https://doi.org/10.3329/dujees.v11i1.63707

concern to avoid the erosion and global-warming induced calamities and engineering proper management. In that case, recording temporal and spatial change and the geometry of the shoreline is crucial for understanding the coastal dynamics and morpho-dynamics of coastal areas (Bheeroo et al., 2016; Del Río et al., 2013; Esteves et al., 2009; Oyedotun, 2014; Stanchev et al., 2018; Tran Thi et al., 2014). Remote sensing and geographic information system (GIS) techniques have become one of the most essential and influential analytical techniques. This technique is associated with spatial and attribute data to produce maps and tables that are extensive, efficient, and time-saving (Mount et al., 2003; Mukherjee et al., 2017; Winterbottom, 2000). The method enables the portrayal of coastal changes and allows the understanding of shoreline dynamics from a temporal series of shoreline positions. Additionally, the technique incorporates multiple factors, like the magnitude and frequency of tides, and shoreline changes from previous coastal events (Brooks et al., 2012; Wolman and Miller, 1960).

The shoreline or bank line alteration to futuristic mitigation processes has been addressed by numerous authors across the globe (Al-Zubieri et al., 2020; Bheeroo et al., 2016; Ciritci and Türk, 2019; El-Sharnouby et al., 2015; Kabuth et al., 2014; Kuleli et al., 2011; Li et al., 2001; Mahmud et al., 2020; Mount et al., 2003; Mukherjee et al., 2017; Murali et al., 2015; Nandi et al., 2016; Özden et al., 2010; Qiao et al., 2018; Rebelo et al., 2009; Sesli et al., 2009; Tran Thi et al., 2014; Zhang et al., 2018), but this is a comparatively contemporary method in Bangladesh. Few endeavors are taken into account for shoreline vulnerability assessment (Islam, et al., 2016a; Islam, et al., 2016b; Islam et al., 2015) and riverbank dynamics (Mahmud et al., 2020), but assessing coastline vulnerability on an island is one of the first approaches.

In this study, the Digital Shoreline Analysis System (DSAS), an ArcGIS extension, has been applied to quantify shoreline change from Landsat images of Moheshkhali island between 1990 and 2020, with an interval of 10 years. This study is indispensable since the government of Bangladesh has approved important mega-projects at Moheshkhali Island, including the country's largest ever infrastructure project, the Moheskhali-Matarbari integrated development project. This is a unique attempt to quantify shoreline change on a coastal island using the DSAS. The study measures and compares erosion and accretion over the study period, specifically identifying the intertidal zone and its shifting, and finally analyzing the trend of shoreline shifting within the Moheshkhali island. The study will also assess the coastal dynamics and will identify the shoreline shifting trends.

STUDY AREA

Moheshkhali is the only hilly offshore island in Bangladesh with a corresponding administrative upazila in Cox's Bazar district. The Moheshkhali channel splits the island from the mainland, Cox's Bazar, and is geographically located between 21°30'0" N and 21°15'0" N latitude and 91°50'0" E to 92°5'0" E longitude, with a total area of 388.50 square kilometers (Fig. 1). The island includes the Matarbari and Shonadia Islands. The island is surrounded by the Chakaria upazila towards the north-east, Cox's Bazar upazila towards the south-east, and the Pekua upazila towards the north. The western and southern parts of the island are bordered by the Bay of Bengal (Fig. 1). The island is featured by a unique geological system towards the eastern cliffy coast of Bangladesh that is characterized by hilly terrain encircled by coastal plain landforms (Islam et al., 2012; Majlis et al., 2013). The island is divided into four sections, which include an active coastal plain, a young coastal plain, an old coastal plain, and a hilly region with piedmont plains (Islam et al., 2011).

Moheshkhali contains hills made of the tertiary rocks of Surma, Tipam, Girujan and Dupi tila formations and the quaternary rocks of the Dihing formation (Majlis et al., 2013). The coastal plains of the area are formed by beach and dune sands, along with alluvial deposits from the late Quaternary (Holocene) age (Alam, 1978). The hills of the area constitute an anticline named the Moheshkhali anticline, which runs in the NNW-SSE direction and plunges towards the NNW (Majlis et al., 2013).

Moheshkhali Island is characterized by two distinct depositional systems: a closed to semi-closed southern regime and an open to closed system in the northern regime (Majlis et al., 2011). It is recorded that the island has been through an accretionary phase at an annual rate of 1.2 km^2 since 1972 (Islam et al., 2011). As a result of changes in land use and land cover patterns, both the southwest coastal plain and the western coastal plain accumulated a large amount of land mass, which in turn contributed to the island's land.

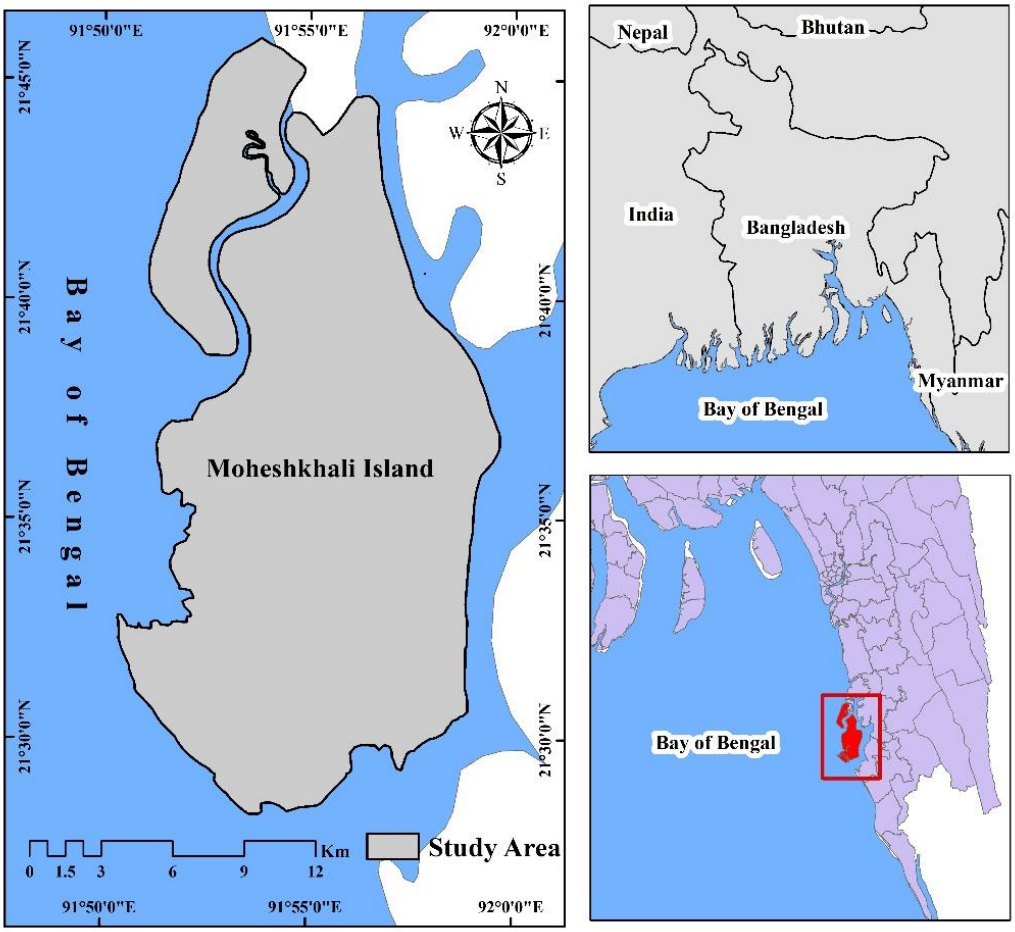

Figure 1: The Location Map of the Study Area

Meteorologically, the research region is mainly characterized by a tropical climate, owing to the influence of the southern monsoon. The area is not adjacent to the estuary of any major river, but rather has a direct link to the Bay of Bengal. Due to its western and southern exposure to the sea, this island is more prone to damage from Cyclones, resulting in changes to the landscape and shifting of the coastline. The native people of the island are dependent upon salt cultivation and shrimp farming as their prime occupations (Islam et al., 2011). The landform and geographical location have an impact on their livelihood and life style.

MATERIALS AND METHODS

Data Source

Multi-temporal Landsat (TM, ETM+, and OLI/TRIS) satellite images for the period between 1990 and 2020 were downloaded to investigate the shoreline dynamics of the Moheshkhali island. Four satellite images were collected from the year of 1990 to 2020 with an interval of 10 years (Table 1). All Landsat images were downloaded from USGS (https://earthexplorer.usgs.gov) and GLOVIS (www.glovis.gov.us) with the condition that the images have less than 5% cloud coverage.

Table 1: Information about Satellite Images

Satellite	Sensor type	Path/row	Acquisition date	Pixel resolution (meter)	Image acquisition time (GMT +6)
Landsat 8	OLI/TRIS	136/45	20/02/2020	30	10:12
Landsat 7	ETM+	136/45	27/02/2010	30	10:05
Landsat 5	TM	136/45	14/12/2000	30	9:46
Landsat 5	TM	136/45	31/12/1900	30	09:50

Data Preparation

In this study, all the satellite images were subjected to georeferenced to the Universal Transverse Mercator (UTM) system in order to achieve spatial accuracy. On the high-resolution Google Earth image, 20 ground control points (GCPs) were carefully selected at landmarks to perform the geometric correction. There was a root-mean-square error (RMSE) of 0.376 pixels at the selected points. The root mean square error (RMSE) demonstrates a strong geometric matching of the images, which was determined by contrasting the fitted-predicted polynomials to coordinate values and coordinates from an independent source (Al-Zubieri et al., 2020; Maanan et al., 2014). This correction procedure is also followed to rectify distortions such as scale fluctuation, tilt, and lens distortion. To reduce distortions such as scale fluctuation, tilt, and lens distortion, a geometric correction procedure is used. Erdas Imagine (version 15) software was used for geometric correction and radiometric enhancement. Further adjustments were made to all of the images, such as histogram equalization, haze and noise reduction, for enhanced visibility (Mahmud et al., 2020).

The final step was to filter each image using an area boundary polygon shapefile defining the circumference of the study.

A semiautomated approach was used for shoreline extraction, as it has been deemed to be superior than automated approach (Dewan et al., 2017; Gupta et al., 2013; Yang et al., 1999). Then a normalized difference vegetation index (NDVI) enacted to classify the images, separating land from waterbodies (Al-Zubieri et al., 2020; Sun et al., 2012). The shorelines were digitized as vector files (polylines) from satellite images in ArcGIS software (version 10.5), with the water boundary indicating the shoreline's edge of the island (Mahmud et al., 2020; Nicoll and Hickin, 2010). Thus, a geo-database was created, containing the shoreline of all the year for subsequent use of DSAS.

Analytical Techniques

For this study, most of the analysis was conducted in a GIS environment using the DSAS interface. For the DSAS extension tool, we used ArcGIS, which was combinedly developed by the United States Geological Survey (USGS) and TPMC Environmental Services (Mahmud et al., 2020; Thieler et al., 2009). The parameters for the temporal shoreline change rate were calculated to assess the shoreline dynamics of Moheshkhali Island.

Shoreline position shifting is calculated automatically using the DSAS technique along user-defined transects. Initially, a 500-meter landward baseline was established parallel to the general direction of the island's shoreline, ensuring that it lay on land with no signs of erosion. A total of 219 transects were generated automatically at intervals of 550m, which is regarded to be minute enough to quantify shoreline changes. Rate of change statistics were generated by intersecting the transects with the historical shoreline positions. Five statistical techniques in DSAS were employed to evaluate the development of the shoreline in the form of accretion/erosion patterns, including the endpoint rate (EPR), linear regression rate (LRR), weighted linear regression rate (WLR), shoreline change envelope (SCE), and net shoreline movement (NSM) (Nassar et al., 2018). NSM and SCE provide shoreline changes in meters, while EPR, LRR, and WLR provide shoreline changes in meters per year.

The EPR is determined by splitting the lateral distance between the oldest and youngest shorelines by the total time that has elapsed. The LLR is a rate-of-change statistic calculated by fitting a least square regression to all shorelines along a given transect. WLR is similar to the LRR approach, except it provides more accurate information at a higher weight. The SCE is a measure of the overall movement of the shoreline, without regard to the specific dates of the movement of any individual shoreline position. The NSM stands for the distance between the oldest and youngest shorelines. Additionally, the standard error, confidence intervals for LRR and WLR, and R square of linear regression were calculated in order to determine the accuracy of the prediction. To justify DSAS outputs, historical shoreline positioning was visually analyzed. A landward movement of the shoreline was interpreted as erosion, denoted by a negative sign, and a seaward movement as accretion, denoted by a positive sign (Anders and Byrnes, 1991).

According to the shoreline change statistics, each coast of Moheshkhali island was divided into multiple erosion/accretion zones. On a color grid map, the manual classification technique in the ArcGIS environment was implemented to illustrate these zones.

Field Investigation

A rigid fieldwork was conducted in the study area to confirm the shoreline change as well as to determine the factors behind the shoreline instability. In order to conduct the field work, a primary zonation map was constructed using the GIS tool. From the zonation map, some active zones were identified, and the survey was taken into account depending on some semi-structured questionnaire. Households and infrastructures were particularly identified using geographic positions. According to the study, a time span of 1990 to 2020 was selected. As a result, individuals over the age of 40 were considered for the interview since they had experienced the change in shoreline over time. Targeted native people have been asked about the alteration of the shoreline and have identified the zones of alteration for the last 30 years. Finally, the data from the in-situ questionnaire survey was compiled and aimed to draw a comparison between the field investigation and the DSAS zonation map. The purpose of this field survey was to verify the output of the DSAS.

RESULT AND DISCUSSION

Shoreline Evaluation

Over a period of 30 years, shoreline evolution identification was carried out along the coastal zone of Moheshkhali Island on the Bay of Bengal coast, at regular intervals (1990, 2000, 2010, and 2020). A number of substantial steps were taken to calculate the total erosion/accretion during the period of 1990–2020. The shoreline evolution over the study period is shown in figure 2, which indicates that the study area exhibits significant erosion and accretion. These evolutions occurred throughout the island's coastal zone, with the most dramatic modifications happening at marine heads in the island's south-western and southern regions (Fig. 2). In the south-west and southern parts of the island, the marine heads were in the form of a semi-crescent, which made them more susceptible to wave action. The geomorphology of these marine heads may have changed as a result of coastal processes like wave energy, longshore currents, and the influence of tides (Al-Zubieri et al., 2020).

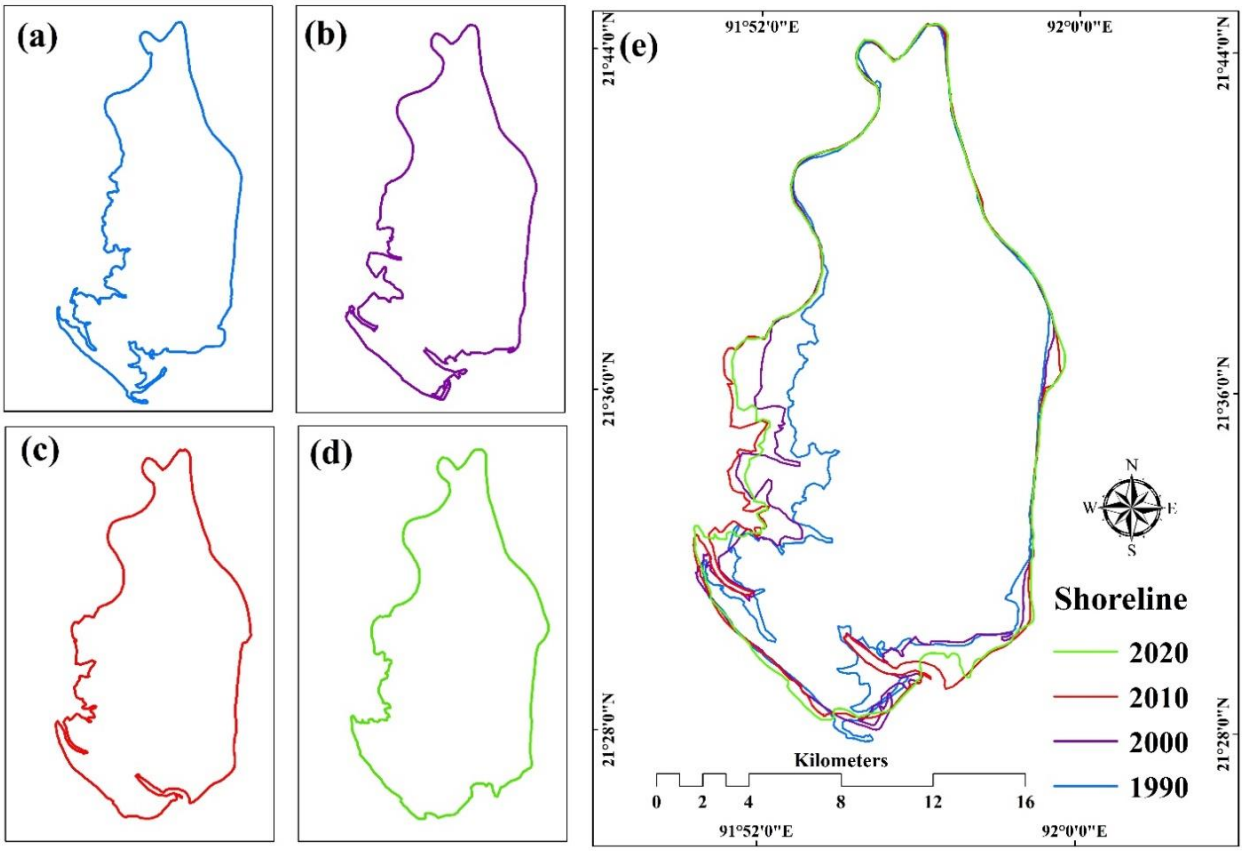

Figure 2: Extracted Shorelines from Different Years; (a) 1990, (b) 2000, (c) 2010, (d) 2020, (e) Combined 1990-2020

The accretion/erosion on the seaward part and southern portion of the shoreline are attributed to the combined impacts of the longshore current and restricting sediment movements carried by the Moheshkhali channel. The channel transported sediments carried along the coast due to the wave action induced by the breaker zone (Al-Zubieri et al., 2020; May and Hansom, 2003). Because of the hydrodynamic conditions in this part of the coast, sediments have accumulated alongshore from north, south direction and creating a seaward movement of the island. This might be related to the low strength of wave energy along this section of the coast, which is attributable to the tidal flats and intertidal zone of the island (Islam et al., 2011). The north and north-eastern parts of the shoreline remain more or less unchanged, but few consecutive erosional and accretional activities are occurring along the coast due to human intervention (Monsur and Kamal, 1994). However, a low rate of accretion has taken place on the northern region of the coast adjacent to the Matarbari channel, where anthropogenic activities have become more extensive, causing more significant accretion. Moreover, this area experienced explosive and broad growth as the Matarbari mega project expanded on the seaward side.

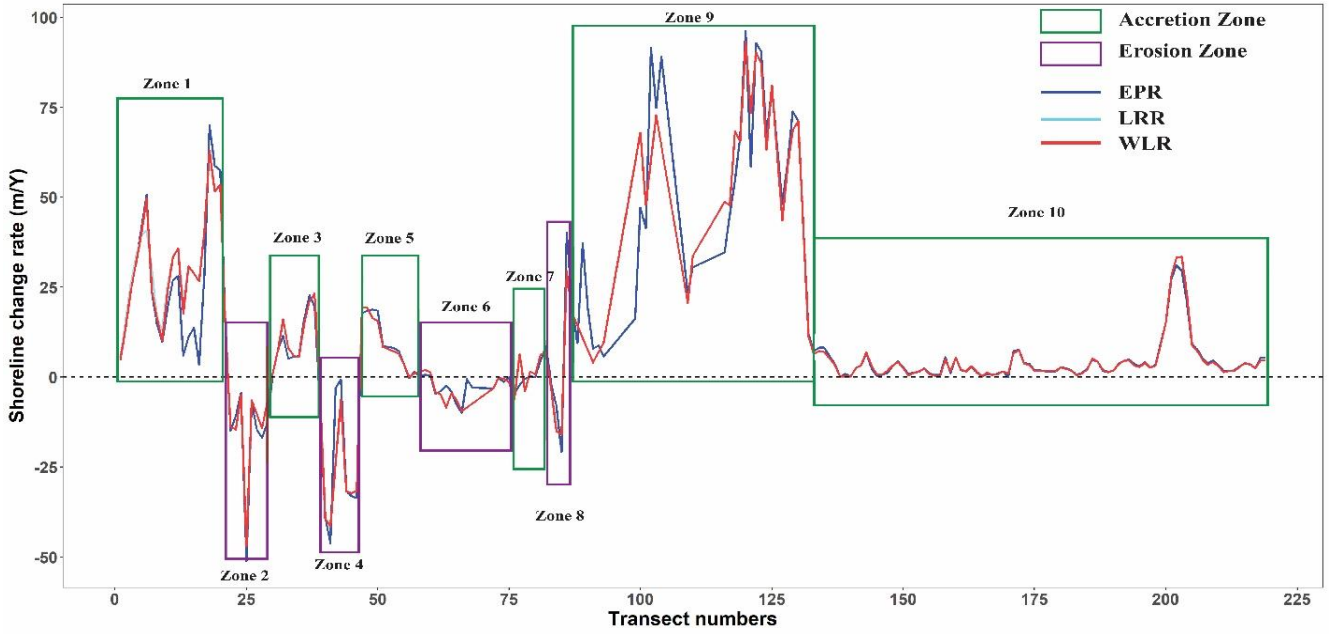

Figure 3: Rates of Shoreline Change in EPR, WLR, and LRR around the Moheshkhali Island

Shoreline Change Rates

As shown in figure 3, EPR, WLR, and LRR distributions along the transects clearly illustrate the high variability in shoreline movement and the dominance of accretion around the island. The shoreline has been divided into 10 distinct zones based on fluctuations in shoreline changes (Fig. 3). Using the NSM and SCE values, a line diagram was constructed (Fig. 4) to test the reliability of the zonation produced from the EPR, WLR, and LRR statistics. The NSM followed a pattern that was similar to that of the EPR, WLR, and LRR, with the exception of SCE, which followed a trend that was the opposite of the others in particular areas. The identical alignments of the NSM and SCE lines indicate accretion, whereas the space between them indicates erosion (Al-Zubieri et al., 2020; Mahmud et al., 2020). Table 2 summarizes shoreline change statistics for the different zones. The average shoreline change rates were used to classify the ten zones into six classes: low erosion (0 to -20m/yr), moderate erosion (-21 to -40m/yr), and high erosion (<-40om/yr); as well as low accretion (+1 to +20m/yr), moderate accretion (+21 to +40m/yr), and high accretion (> +40m/yr) in order to depict the risk level across the study area. This categorization was dependent on the probable socio-environmental consequences and the shoreline vulnerability parameters specified by Mahapatra et al. (2014).

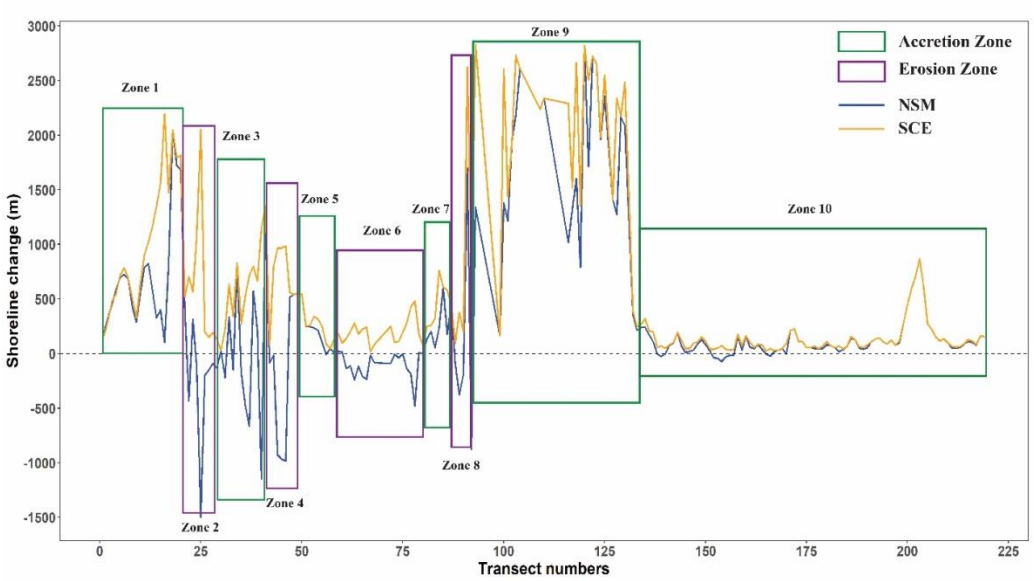

Figure 4: Shoreline Change in NSM and SCE around the Moheshkhali Island

During the study period, it is illustrated that six of the ten zones of the shoreline were accretion dominant (Table 2). These zones include zone Z9, which was classified as a high accretion zone, zone Z1, which was classified as a moderate accretion zone, and zones Z3, Z5, Z7, and Z10 were categorized as low accretion dominat zones. Besides, zones Z2, Z4, Z6, and Z8 were categorized as erosion dominant zones (Table 2). During the study period, shorelines along all transects accreted at a rate of about 86 m/year on average (Table 3).

The coefficients of determination for all zones on the shoreline were high except for Z1, Z8, and Z9 (Table 2). A very high R^2 (>0.80) suggests excellent prediction of the shoreline change rate (Mahmud et al., 2020). In the case of Z1 (.42), Z8 (.60), and R9 (.30), the low R^2 values may reflect the high level of dynamic nature of these zones, which are subject to high erosion and accretion.

Historically, the shoreline position changes of Z9 and Z1 had a considerable impact between 1990 and 2010, gained great amounts of land. There was no erosion until 2010, when a slow rate of erosion began, and for a further 10 years erosion continued. Similar to Z9 and Z1, Z2, and Z3 were subjected to erosion and accretion phases. The low rate of accretion observed in zone Z10 since 1990 may explain the high R^2 values (Table 2). This could also explain the shoreline stability in Z10. The field investigation results and social survey results obtained in Zones Z1, Z2, Z3, Z9, and Z10 supported the shoreline change rates calculated from the DSAS. According to locals interviewed, Z1 and Z9 were undergoing accretion until 2020. Within a very short period of time, it had accreted a significant amount of land. Participants also reported that land is currently being added to the area at a rate of nearly 70-80 meters per year. Local residents report that Z10 has maintained a stable condition with a low rate of accretion, similar to the DSAS output. In many places, shoreline protection measures (mangrove plantations, artificial structures) are being implemented to reduce shoreline erosion. However, during catastrophic events, such as spring tides, storm surges, cyclones, etc., the failure of those protection measures accelerated shoreline erosion (Mahmud et al., 2020).

Table 2: Summary of Zone-wise Shoreline Statistics for Moheshkhali Island. Shoreline Changes are Expressed in m/year for EPR, WLR, and LRR and in m for NSM and SCE

Zone	Statistical Parameters	No. of transect	Mean	Minimum	Maximum	Average R^2	Remarks
	EPR		26.27	3.56	69.97		
	LRR		30.07	4.75	62.99	0.42	Moderate
Z1	WLR	21	30.59	4.75	62.99	0.32	accretion
	NSM		695.98	104.47	2050.49		
	SCE		997.28	159.43	2193.5		
	EPR		-16.54	-51.16	-4.32		
	LRR		-16.82	-47.01	-4.83	0.99	Low erosion
Z2	WLR	8	-16.82	-47.01	-4.83	0.84	
	NSM		-289.92	-1499.32	314.23		
	SCE		634.65	130.69	2051.91		
	EPR		0.19	-46.19	22.75		
	LRR		1.53	-41.52	23.21	0.99	Low
Z3	WLR	12	1.53	-41.52	23.21	0.89	accretion
	NSM		40.12	-1145.69	1353.81		
	SCE		626.99	26.11	1353.81		
	EPR		-9.39	-33.58	18.45		
	LRR		-10.57	-32.26	19.3	0.98	Low erosion
Z4	WLR	7	-10.57	-32.26	19.3	0.83	
	NSM		-275.023	-984.02	540.64		
	SCE		699.99	86.31	984.02		
	EPR		6.84	-0.3	18.79		
	LRR		6.33	-0.08	16.41	0.99	Low
Z5	WLR	11	6.33	-0.08	16.41	0.90	accretion
	NSM		200.47	-8.79	550.74		
	SCE		268.79	43.38	550.74		
	EPR		-2.64	-9.97	0.43		
	LRR		-2.70	-9.42	6.35	0.83	Low erosion
Z6	WLR	21	-2.70	-9.42	6.35	0.85	
	NSM		-115.412	-479.26	12.57		
	SCE		197.38	17.08	479.26		
	EPR		3.78	-20.83	40.12		
	LRR		1.35	-16.02	29.32	0.95	Low
Z7	WLR	6	1.35	-16.02	29.32	0.74	accretion
	NSM		234.72	-51.92	610.57		
	SCE		463.565	247.34	762.15		
	EPR		-7.84	-37.23	19.54		
	LRR		10.92	4.08	17.76	0.60	Low erosion
Z8	WLR	6	10.92	4.08	17.76	0.58	
	NSM		99.14	-880.07	1696.89		
	SCE		769.12	95.81	2622.79		
	EPR		59.10	5.75	96.32		
	LRR		60.63	9.69	93.23	0.30	High
Z9	WLR	39	60.63	9.69	93.23	0.41	accretion
	NSM		1796.42	-164.89	2822.82		
	SCE		2189.54	164.89	2828.87		
	EPR		4.39	0.09	31.05		
	LRR		4.38	0.12	33.48	0.99	Low
Z10	WLR	88	4.38	0.12	33.48	0.96	accretion
	NSM		117.80	-72.3	867.42		
	SCE		139.84	23.4	867.42		

A colored gird shoreline erosion/accretion zone map of the Moheshkhali Island is shown in figure 5 which provides a vulnerability zonation of the shoreline of the island. This map also illustrates the relative stability of the shoreline zone of Moheshkhali Island. According to the figure 5, zones Z2, Z4, Z6, and Z8 pay more attention due to the active erosion processes. This zone the island demands additional surveillance in order to protect the coast, like the installation of wave breaker zone in the open sea and different coastal structures (Al-Zubieri et al., 2020). Zones Z1, Z3, Z5, Z7, and Z9 are accretion dominant, whereas Z10 is more stable. In this study, shoreline appears to be extremely dynamic and spatially variable, even to the point that accretion can turn into erosion within a very short span of time. This highly dynamic nature of the shoreline, i.e., rapid erosion and accretion, can be attributed to several factors. The alteration of the shoreline of the island is directly affected by wave action, longshore current effects, engineering features of shore sediments, and human intervention, which are the consequences of climatic change and sea-level rise. The results indicated that the zones dominated by erosion were distributed in the seaward direction of the island, whereas the major accretion zones are situated in the reverse direction, toward the river area (Fig. 5). Likewise, the coastal low-lying areas across the globe, the coastal area of Bangladesh is also severely affected by the result of climate change sea-level rise. This clearly demonstrates that wave action and current dynamics changed between 1990 and 2020 because of sea-level rise, which may be the prime driving factor in causing the erosion and accretion zones of the studied shoreline.

Table 3: Average Rates of Shoreline Change over the Last 30 Years

Parameters analyzed	Shoreline change rate (m/yr)
EPR	88.99
LRR	85.12
WLR	85.64
Average	86.58

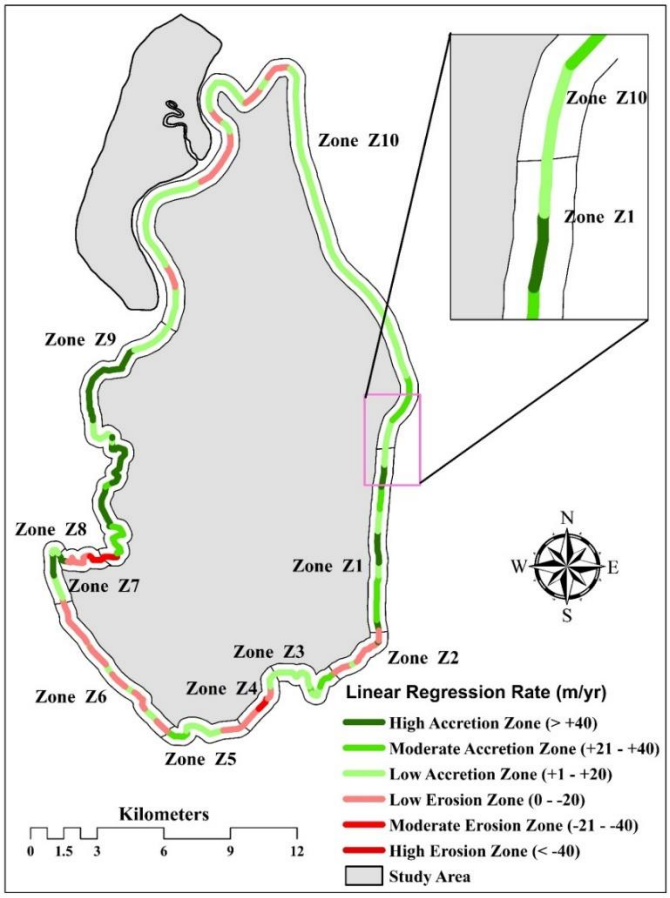

Figure 5: Shoreline Evolution Zone Map of the Moheshkhali Island

CONCLUSIONS

The shoreline evaluation of Moheshkhali Island on the Bay of Bengal coast, in the Cox's Bazar district of Chittagong division, was efficiently delineated and evaluated between the 1990 and 2020 frames, employing GIS techniques and automated calculations using DSAS. Over the course of 30 years, multi-temporal 30m satellite images were used to study shoreline change throughout the coastal area of the island. Four shoreline positions were retrieved by DSAS in 1990, 2000, 2010, and 2020. Moheshkhali Island experienced consecutive erosion and accretion by the combined effects of climate change and sea-level rise. Thus, significant fluctuations in coastline area were identified by the study. The simulated values from EPR, WLR, and LRR delineated six accretion zones where the sediments carried by the oceanic water are accumulated. Moreover, four distinct zones were identified that are highly vulnerable and are subjected to subsequent erosion, which needs to be protected by relevant infrastructural developments. In both cases, the values were verified by using NSM, SCE values, and the line diagram method. The study found that the south and southwest zones of the island accreted at a higher rate with respect to the north and north-eastern zones. Some minute alterations were tracked down in the northern and north-eastern zones of the study area. In the investigated area, disintegration was attributed to different factors, including high sediment discharge through the Moheshkhali channel, longshore transport along the coast, and the impact of strong waves. A wide range of other factors also contribute to the highly dynamic nature of shorelines, including climate change, windy storms, variations in bank materials, and human activities. In addition, the coastal region of Bangladesh experiences catastrophic natural events, especially cyclones, every year during the pre-monsoon season, and significant diurnal tidal effects also take place during the wet season. Despite the fact that the images were collected during the dry season, which reduces tidal influences, we were unable to apply tidal adjustments due to a lack of tidal data at the time of image collection. The results could have been more comprehensive if higher-resolution images had been deployed. Moreover, a shorter temporal change could have yielded more precise data output from 1990 to 2020. It suggested that as the shoreline of the studied area accreted substantially, this required greater supervision. Hence, this study may be incorporated as baseline studies for the futuristic shoreline dynamics and may provide additional insights while evaluating the hydrogeologic and geotechnical properties of the shoreline. The study enables the associated authorities and policymakers to take zone-based development and protection measures to alleviate the environmental and socioeconomic complications.

ACKNOWLEDGEMENT

The authors are grateful to the University Grants Commission (UGC) and to the University of Dhaka, Bangladesh for funding the study (fiscal year: 2019-2020).

REFERENCES

Alam, M.K., 1978. Probable scope of hydrological and other developments in Moheskhali Island and its adjoining areas. 4th Annual Conference, Bangladesh Geological Society, Dhaka, Proceedings, 51-57.

Al-Zubieri, A.G., Ghandour, I.M., Bantan, R.A. Basaham, A.S., 2020. Shoreline evolution between Al Lith and Ras Mahāsin on the Red Sea coast, Saudi Arabia using GIS and DSAS techniques. Journal of the Indian Society of Remote Sensing 48(10), 1455–1470. https://doi.org/10.1007/s12524-020-01169-6

Ali, A., 1996. Vulnerability of Bangladesh to climate change and sea level rise through tropical cyclones and storm surges. In: Climate change vulnerability and adaptation in Asia and the Pacific, pp. 171–179. Springer. https://doi.org/10.1007/978-94-017-1053-4_16

Anders, F.J., Byrnes, M.R., 1991. Accuracy of shoreline change rates as determined from maps and aerial photographs. Shore and Beach 59(1), 17–26.

Bheeroo, R.A., Chandrasekar, N., Kaliraj, S., Magesh, N.S., 2016. Shoreline change rate and erosion risk assessment along the Trou Aux Biches–Mont Choisy beach on the northwest coast of Mauritius using GIS-DSAS technique. Environmental Earth Sciences 75(5), 444. https://doi.org/10.1007/s12665-016-5311-4

Brooks, S.M., Spencer, T., Boreham, S., 2012. Deriving mechanisms and thresholds for cliff retreat in soft-rock cliffs under changing climates: rapidly retreating cliffs of the Suffolk coast, UK. Geomorphology 153, 48–60.

https://doi.org/10.1016/j.geomorph.2012.02.007

Choudhury, A.M., Haque, M.A., Quadir, D.A., 1997. Consequences of global warming and sea level rise in Bangladesh. Marine Geodesy 20(1), 13–31. https://doi.org/10.1080/01490419709388092

Ciritci, D., Türk, T.. 2019. Automatic detection of shoreline change by geographical information system (GIS) and remote sensing in the Göksu delta, Turkey. Journal of the Indian Society of Remote Sensing 47(2), 233–243. https://doi.org/10.1007/s12524-019-00947-1

Del Río, L., Gracia, F.J., Benavente, J., 2013. Shoreline change patterns in sandy coasts. A case study in SW Spain. Geomorphology 196, 252–266. https://doi.org/10.1016/j.geomorph.2012.07.027

Dewan, A., Corner, R., Saleem, A., Rahman, M.M., Haider, M.R., Rahman, M.M., Sarker, M.H., 2017. Assessing channel changes of the Ganges-Padma river system in Bangladesh using Landsat and hydrological data. Geomorphology 276, 257–279. https://doi.org/10.1016/j.geomorph.2016.10.017

El-Sharnouby, B.A., El-Alfy, K.S., Rageh, O.S., El-Sharabasy, M.M., 2015. Coastal changes along Gamasa beach, Egypt. J Coast Zone Manag 17, 393-404.

Esteves, L.S., Williams, J.J., Nock, A., Lymbery, G., 2009. Quantifying shoreline changes along the Sefton coast (UK) and the implications for research-informed coastal management. Journal of Coastal Research SI56, 602–606.

Gupta, N., Atkinson, P.M., Carling, P.A., 2013. Decadal length changes in the fluvial planform of the River Ganga: bringing a mega-river to life with Landsat archives. Remote Sensing Letters 4(1), 1–9. https://doi.org/10.1080/2150704X.2012.682658

Islam, M.A., Hasan, M., Peas, M.H., Naime, M.A., Gazi, M.Y., Rahman, M.M., 2016. Shoreline vulnerability assessment in an offshore island (Sandwip), Bangladesh – an appraisal of geospatial techniques. Dhaka University Journal of Earth and Environmental Sciences 5(December), 51–60.

Islam, M.A., Hossain, M.S., Murshed, S., 2015. Assessment of coastal vulnerability due to sea level change at Bhola Island, Bangladesh: using geospatial techniques. Journal of the Indian Society of Remote Sensing 43(3), 625–637.

Islam, M.A., Majlis, A.B.K., Rashid, M.B., 2011. Changing face of Bangladesh coast. In: Abstract volume, National seminar on Bangladesh Coast: Geology, Hazards and Resources. Dhaka, Bangladesh.

Islam, M.A., Mitra, D., Dewan, A., Akhter, S.H., 2016. Coastal multi-hazard vulnerability assessment along the Ganges deltaic coast of Bangladesh–A geospatial approach. Ocean & Coastal Management 127, 1–15.

Islam, M.S., Tusher, T.R., Mustafa, M., Mahmud, S., 2012. Effects of solid waste and industrial effluents on water quality of Turag river at Konabari industrial area, Gazipur, Bangladesh. Journal of Environmental Science and Natural Resources 5(2), 213–218.

Kabuth, A.K., Kroon, A., Pedersen, J.B.T., 2014. Multidecadal shoreline changes in Denmark. Journal of Coastal Research 30(4), 714–728. https://doi.org/10.2112/JCOASTRES-D-13-00139.1

Karim, M.F., Mimura, N., 2008. Impacts of climate change and sea-level rise on cyclonic storm surge floods in Bangladesh. Global Environmental Change 18(3), 490–500. https://doi.org/10.1016/j.gloenvcha.2008.05.002

Kuleli, T., Guneroglu, A., Karsli, F., Dihkan, M., 2011. Automatic detection of shoreline change on coastal Ramsar wetlands of Turkey. Ocean Engineering 38(10), 1141–1149. https://doi.org/10.1016/j.oceaneng.2011.05.006

Li, R., Liu, J.-K., Felus, Y., 2001. Spatial modeling and analysis for shoreline change detection and coastal erosion monitoring. Marine Geodesy 24(1), 1–12. https://doi.org/10.1080/01490410121502

Maanan, M., Ruiz-Fernandez, A.C., Maanan, M., Fattal, P., Zourarah, B., Sahabi, M., 2014. A long-term record of land use change impacts on sediments in Oualidia lagoon, Morocco. International Journal of Sediment Research 29(1), 1–10. https://doi.org/10.1016/S1001-6279(14)60017-2

Mahapatra, M., Ratheesh, R., Rajawat, A.S., 2014. Shoreline change analysis along the coast of

South Gujarat, India, using digital shoreline analysis system. Journal of the Indian Society of Remote Sensing 42(4), 869–876. https://doi.org/10.1007/s12524-013-0334-8

Mahmud, M.I., Mia, A.J., Islam, M.A., Peas, M.H., Farazi, A.H., Akhter, S.H., 2020. Assessing bank dynamics of the Lower Meghna River in Bangladesh: an integrated GIS-DSAS approach. Arabian Journal of Geosciences 13(14). https://doi.org/10.1007/s12517-020-05514-4. https://doi.org/10.1007/s11414-013-9386-3

Majlis, A.B., Islam, M., Khasru, M.A., Ahsan, M.K., 2011. Protectred to open basin depositional system: an appraisal for the quaternary evolution of the Moheshkhali-Kutubdia coastal plain, Bangladesh, In: Abstract volume. National seminar on Bangladesh Coast: Geology, Hazards and Resources. Dhaka, Bangladesh.

Majlis, A.B.K., Islam, M.A., Khasru, M.H., Ahsan, M.K., 2013. Protected to open basin depositional system: An appraisal for the Late Quaternary evolution of the Moheshkhali-Kutubdia coastal plain, Bangladesh. Bangladesh Journal of Geology 26, 64–77.

Mallick, F., Rahman, A., 2013. Cyclone and tornado risk and reduction approaches in Bangladesh. In: Disaster risk reduction approaches in Bangladesh, pp. 91–102. Springer.

May, V.J., Hansom, J.D., 2003. Coastal geomorphology of Great Britain (Vol. 28). Joint Nature Conservation Committee.

Monsur, M.H., Kamal, A., 1994. Holocene sea-level changes along the Maiskhali and Cox's Bazar-Teknaf Coast of the Bay of Bengal. The Journal of NOAMI 11(1), 15–21.

Mount, N.J., Louis, J., Teeuw, R.M., Zukowskyj, P.M., Stott, T., 2003. Estimation of error in bankfull width comparisons from temporally sequenced raw and corrected aerial photographs. Geomorphology 56(1–2), 65–77. https://doi.org/10.1016/S0169-555X(03)00046-1

Mukherjee, R., Bilas, R., Biswas, S.S., Pal, R., 2017. Bank erosion and accretion dynamics explored by GIS techniques in lower Ramganga river, Western Uttar Pradesh, India. Spatial Information Research 25(1), 23–38. https://doi.org/10.1007/s41324-016-0074-2

Murali, R.M., Dhiman, R., Choudhary, R., Seelam, J.K., Ilangovan, D., Vethamony, P., 2015. Decadal shoreline assessment using remote sensing along the central Odisha coast, India. Environmental Earth Sciences 74(10), 7201–7213. https://doi.org/10.1007/s12665-015-4698-7

Nandi, S., Ghosh, M., Kundu, A., Dutta, D., Baksi, M., 2016. Shoreline shifting and its prediction using remote sensing and GIS techniques: a case study of Sagar Island, West Bengal (India). Journal of Coastal Conservation 20(1), 61–80. https://doi.org/10.1007/s11852-015-0418-4

Nassar, K., Fath, H., Mahmod, W.E., Masria, A., Nadaoka, K., Negm, A., 2018. Automatic detection of shoreline change: case of North Sinai coast, Egypt. Journal of Coastal Conservation, 22(6) 1057–1083. https://doi.org/10.1007/s11852-018-0613-1

Nicoll, T.J., Hickin, E.J., 2010. Planform geometry and channel migration of confined meandering rivers on the Canadian prairies. Geomorphology 116(1–2), 37–47. https://doi.org/10.1016/j.geomorph.2009.10.005

Oyedotun, T.D.T., 2014. Shoreline geometry: DSAS as a tool for historical trend analysis. Geomorphological Techniques 3(2.2), 1–12.

Özden, Ö., Ulusoy, Ş., Erkan, N., 2010. Study on the behavior of the trace metal and macro minerals in Mytilus galloprovincialis as a bioindicator species: the case of Marmara Sea, Turkey. Journal Für Verbraucherschutz Und Lebensmittelsicherheit 5(3), 407–412.

Qiao, G., Mi, H., Wang, W., Tong, X., Li, Z., Li, T., Hong, Y., 2018. 55-year (1960–2015) spatiotemporal shoreline change analysis using historical DISP and Landsat time series data in Shanghai. International Journal of Applied Earth Observation and Geoinformation 68, 238–251.

Rebelo, L.-M., Finlayson, C.M., Nagabhatla, N., 2009. Remote sensing and GIS for wetland inventory, mapping and change analysis. Journal of Environmental Management 90(7), 2144–2153. https://doi.org/10.1016/j.jenvman.2007.06.027

Sesli, F.A., Karsli, F., Colkesen, I., Akyol, N., 2009. Monitoring the changing position of coastlines using aerial and satellite image data: an example from the eastern coast of Trabzon, Turkey. Environmental Monitoring and Assessment 153(1), 391–403.

https://doi.org/10.1007/s10661-008-0366-7

Stanchev, H., Stancheva, M., Young, R., Palazov, A., 2018. Analysis of shoreline changes and cliff retreat to support Marine Spatial Planning in Shabla Municipality, Northeast Bulgaria. Ocean & Coastal Management 156, 127–140. https://doi.org/10.1016/j.ocecoaman.2017.06.011

Sun, F., Sun, W., Chen, J., Gong, P., 2012. Comparison and improvement of methods for identifying waterbodies in remotely sensed imagery. International Journal of Remote Sensing 33(21), 6854–6875. https://doi.org/10.1080/01431161.2012.692829

Thieler, E.R., Himmelstoss, E.A., Zichichi, J.L., Ergul, A., 2009. The Digital Shoreline Analysis System (DSAS) version 4.0-an ArcGIS extension for calculating shoreline change. US Geological Survey. https://doi.org/10.3133/ofr20081278

Tran Thi, V., Tien Thi Xuan, A., Phan Nguyen, H., Dahdouh-Guebas, F., Koedam, N., 2014. Application of remote sensing and GIS for detection of long-term mangrove shoreline changes in Mui Ca Mau, Vietnam. Biogeosciences 11(14), 3781–3795. https://doi.org/10.5194/bg-11-3781-2014

Winterbottom, S.J., 2000. Medium and short-term channel planform changes on the Rivers Tay and Tummel, Scotland. Geomorphology 34(3–4), 195–208.

Wolman, M.G., Miller, J.P., 1960. Magnitude and frequency of forces in geomorphic processes. The Journal of Geology 68(1), 54–74. https://doi.org/10.1086/626637

Yang, X., Damen, M.C.J., Van Zuidam, R.A., 1999. Satellite remote sensing and GIS for the analysis of channel migration changes in the active Yellow River Delta, China International Journal of Applied Earth Observation and Geoinformation 1(2), 146–157. https://doi.org/10.1016/S0303-2434(99)85007-7

Zhang, X., Yang, Z., Zhang, Y., Ji, Y., Wang, H., Lv, K., Lu, Z., 2018. Spatial and temporal shoreline changes of the southern Yellow River (Huanghe) Delta in 1976–2016. Marine Geology 395, 188–197. https://doi.org/10.1016/j.margeo.2017.10.006